doi:10.1038/nature07427

LETTERS

Generation of a prostate from a single adult stem cell

Kevin G. Leong[1], Bu-Er Wang[1], Leisa Johnson[1] & Wei-Qiang Gao[1]

The existence of prostate stem cells (PSCs) was first postulated from the observation that normal prostate regeneration can occur after repeated cycles of androgen deprivation and replacement in rodents[1]. Given the critical role of PSCs in maintaining prostate tissue integrity and their potential involvement in prostate tumorigenesis[2], it is important to define specific markers for normal PSCs. Several cell-surface markers have been reported to identify candidate PSCs, including stem cell antigen-1 (Sca-1, also known as Ly6a), CD133 (Prom1) and CD44 (refs 3–10). However, many non-PSCs in the mouse prostate also express these markers and thus identification of a more defined PSC population remains elusive. Here we identify CD117 (c-kit, stem cell factor receptor) as a new marker of a rare adult mouse PSC population, and demonstrate that a single stem cell defined by the phenotype Lin$^-$Sca-1$^+$CD133$^+$CD44$^+$CD117$^+$ can generate a prostate after transplantation *in vivo*. CD117 expression is predominantly localized to the region of the mouse prostate proximal to the urethra and is upregulated after castration-induced prostate involution—two characteristics consistent with that of a PSC marker. CD117$^+$ PSCs can generate functional, secretion-producing prostates when transplanted *in vivo*. Moreover, CD117$^+$ PSCs have long-term self-renewal capacity, as evidenced by serial isolation and transplantation *in vivo*. Our data establish that single cells in the adult mouse prostate with multipotent, self-renewal capacity are defined by a Lin$^-$Sca-1$^+$CD133$^+$CD44$^+$CD117$^+$ phenotype.

The mouse prostate consists of four pairs of lobes (dorsal, lateral, ventral and anterior lobes) with each divided into three regions relative to the urethra (distal, intermediate and proximal regions; Fig. 1a)[11]. A recent model suggests that the proximal region of prostatic ducts may constitute the stem cell niche in the mouse prostate[12–14]. Using this model, we postulated that new PSC markers would have greater expression in the proximal region relative to the remaining regions of the prostate. We therefore divided wild-type prostates into distal, intermediate and proximal regions and performed quantitative reverse transcriptase polymerase chain reaction (qRT–PCR) analysis for stem cell markers. Four cell-surface

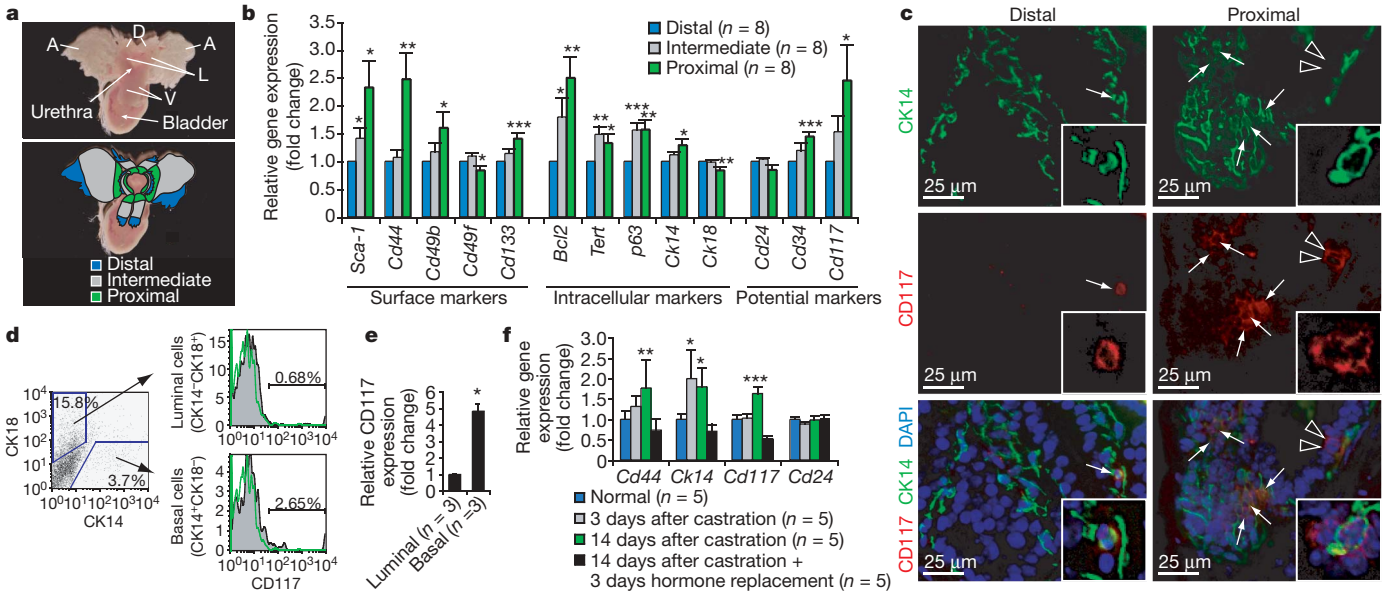

Figure 1 | CD117 is preferentially expressed in the proximal region of the mouse prostate. a, Intact prostate from an adult C57BL/6 mouse. Four pairs of lobes (dorsal (D), lateral (L), ventral (V) and anterior (A)) are shown (top panel). The bottom panel indicates distal, intermediate and proximal regions for each prostatic lobe, relative to the urethra. **b**, qRT–PCR for gene expression in the different regions of the adult C57BL/6 prostate, normalized to the distal region. Statistical comparisons with distal region: $*P < 0.05$; $**P < 0.01$; $***P < 0.001$. **c**, Immunofluorescent staining for CK14 (green) and CD117 (red) in distal and proximal regions of an adult C57BL/6 prostate, counterstained with 4,6-diamidino-2-phenylindole (DAPI; blue). Arrows indicate CD117$^+$CK14$^+$ cells and arrowheads indicate CD117$^+$CK14$^-$ cells. Insets show magnified cells. **d**, Flow cytometric analysis of adult C57BL/6 prostate cells triple-stained with CK14, CK18 and CD117, and gated on basal (CK14$^+$CK18$^-$) and luminal (CK14$^-$CK18$^+$) populations. Green line shows control labelling. Dot plots indicate the percentage of basal and luminal cells and histograms indicate the percentage of CD117$^+$ cells in each of the basal and luminal populations. **e**, Quantification of relative CD117 expression in the basal and luminal compartments determined by flow cytometry; $*P = 0.01$. **f**, Microarray analysis of gene expression in adult C57BL/6 prostates (normal, 3 days after castration, 14 days after castration, and 14 days after castration with 3 days of hormone replacement). Data are expressed as the fold change relative to normal. Statistical comparisons with hormone replacement: $*P < 0.05$; $**P < 0.01$; $***P < 0.0001$. All bars represent the mean and s.e.m.

[1]Department of Molecular Biology, Genentech, Inc., 1 DNA Way, South San Francisco, California 94080, USA.

©2008 Macmillan Publishers Limited. All rights reserved

markers (Sca-1, CD44, CD49b (also known as Itga2) and CD133) all of which are known markers of PSCs[3–8], and three intracellular stem-cell markers (Bcl2, telomerase reverse transcriptase (Tert) and p63) showed preferential expression in the proximal region (Fig. 1b and Supplementary Fig. 1a), thus confirming the validity of this assay. The fact that CD44, CD49b, CD133, Bcl2, Tert and p63 are all prostatic basal markers[4–6,8,15,16] suggests that basal markers, relative to luminal markers, may be expressed at increased levels in the proximal region. Consistently, the basal marker cytokeratin 14 (CK14, also known as Krt14) but not the luminal marker CK18 (Krt18) showed preferential expression in the proximal region (Fig. 1b). These data support the previous suggestion that PSCs may constitute a subpopulation of basal cells[8,9].

We next assessed the expression levels of stem cell-surface markers that were not previously reported to identify normal PSCs. CD34 and CD117, but not CD24, were predominantly expressed in the proximal region (Fig. 1b). Because CD117 showed greater differential expression between the proximal and distal regions compared to CD34 (Fig. 1b), we focused on CD117 as a potential PSC marker. Immunostaining confirmed a basal $CD117^+CK14^+$ population with a predominantly proximal expression pattern (Fig. 1c). A proximal $CD117^+CK14^-$ population, however, was also observed (Fig. 1c) with subsequent analysis identifying a luminal $CD117^+CK18^+$ population (Supplementary Fig. 1b). We next performed flow cytometry with triple labelling for CK14, CK18 and CD117 (Fig. 1d). Although $CD117^+$ cells were enriched in the basal compartment (Fig. 1e) these findings indicated that $CD117^+$ cells were not exclusively localized to either the basal or luminal compartments. Moreover, CD117 expression was not confined to a particular prostatic lobe. Instead, CD117—along with CD44, CD49b and CD133—was expressed in all four pairs of lobes, with prominent expression detected in the dorsal prostate (Supplementary Fig. 1c, d). CD117 therefore has an expression profile that is similar to that of known PSC markers.

Although normal PSCs are androgen-independent and survive castration, they remain androgen-responsive and effect prostate regeneration after hormone replacement[1]. If normal PSCs expressed CD117, we postulated that CD117 expression would increase after castration (owing to stem-cell enrichment) and decrease after hormone replacement (owing to differentiated cell expansion). Indeed, CD117, CK14 and CD44, but not CD24, showed this pattern (Fig. 1f and Supplementary Fig. 1e), further indicating that the expression of CD117 is compatible with that of a normal PSC marker.

To provide functional evidence that the $CD117^+$ population is enriched for PSCs, we prepared $CD117^{+/-}$ fractions (Supplementary Fig. 2) and performed prostate colony formation assays *in vitro*[13]. $CD117^+$ cells (but not $CD117^-$ cells) gave rise to several lumen-containing colonies (Fig. 2a). Although this *in vitro* assay suggests that the $CD117^+$ population contains PSCs, the ability of $CD117^+$ cells to generate prostates *in vivo* is an essential assessment of the stem-cell phenotype. Using an *in vivo* prostate generation system[17,18] $CD117^{+/-}$ fractions from C57BL/6 mouse donors were combined with rat embryonic urogenital sinus mesenchymal (UGM) stromal cells and implanted under the renal capsule of athymic nu/nu mouse hosts. Although $CD117^-$ cells remained viable under the renal capsule (Supplementary Fig. 3), grafts of $CD117^-$ cells were small, opaque and similar to grafts of UGM cells alone in their inability to generate prostates (prostate generation frequency (pgf) = 1/10; Fig. 2b, c). In contrast, $CD117^+$ grafts were large, vascularized and translucent (pgf = 10/12; Fig. 2b, c). Histological examination of $CD117^+$ grafts demonstrated a branching morphology (Fig. 2d) with epithelial tubules composed of basal (CK14; Fig. 2e) and luminal (CK18; Fig. 2e) cell lineages. Rare neuroendocrine cells—identified as solitary synaptophysin $(Syp)^+$ cells in the basal compartment of wild-type mouse prostates (Supplementary Fig. 4)[19]—were observed in several prostatic ducts and acini, within the same and across multiple implants (Fig. 2f). $CD117^+$ grafts also expressed the prostate-specific proteins probasin (Pbsn)[20] (Fig. 2g) and Nkx3-1 (ref. 21; Fig. 2h), indicating functional prostate generation. Using a mouse β1 integrin (also known as Itgb1)-specific antibody, we verified that $CD117^+$ grafts were of mouse origin and not due to contaminating rat epithelial cells from the UGM stromal cell preparations (Fig. 2i). Furthermore, we confirmed that the generated prostates were derived from transplanted $CD117^+$ donor cells using an MHC class I

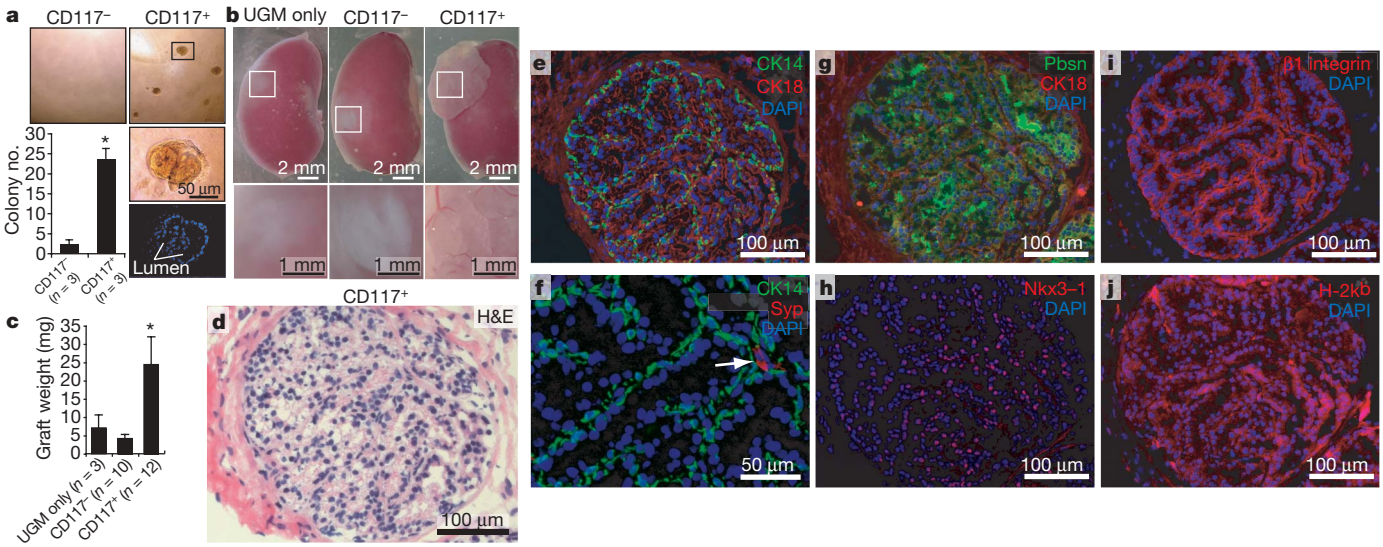

Figure 2 | The $CD117^+$ population enriches for normal adult prostate stem cells. **a**, Colony forming abilities of $CD117^-$ and $CD117^+$ cell populations from adult C57BL/6 prostates. The boxed area is shown enlarged in the middle right image, and a DAPI-stained confocal image demonstrating lumen formation is shown in the bottom right image. Data are from three independent experiments; $*P < 0.0001$. **b**, Prostate generation capacities of UGM only, $CD117^-$ and $CD117^+$ implants 2 months after renal capsule implantation. The boxed areas in the top panels are shown enlarged in the bottom panels. **c**, Quantification of graft weight 2 months after renal capsule implantation. Data are from five independent experiments. *, $CD117^+$ versus $CD117^-$: $P = 0.02$; $CD117^+$ versus UGM only: $P = 0.03$. Data are mean and s.e.m. **d–j**, Histological analyses of serial sections of a $CD117^+$ graft stained for (**d**) haematoxylin and eosin (H&E), (**e**) CK14 (green), CK18 (red) and DAPI (blue), (**f**) CK14 (green), Syp (red) and DAPI (blue), (**g**) Pbsn (green), CK18 (red) and DAPI (blue), (**h**) Nkx3-1 (red) and DAPI (blue), (**i**) β1 integrin (red) and DAPI (blue), (**j**) H-$2k^b$ (red) and DAPI (blue). Arrow indicates a Syp^+ cell.

©2008 Macmillan Publishers Limited. All rights reserved

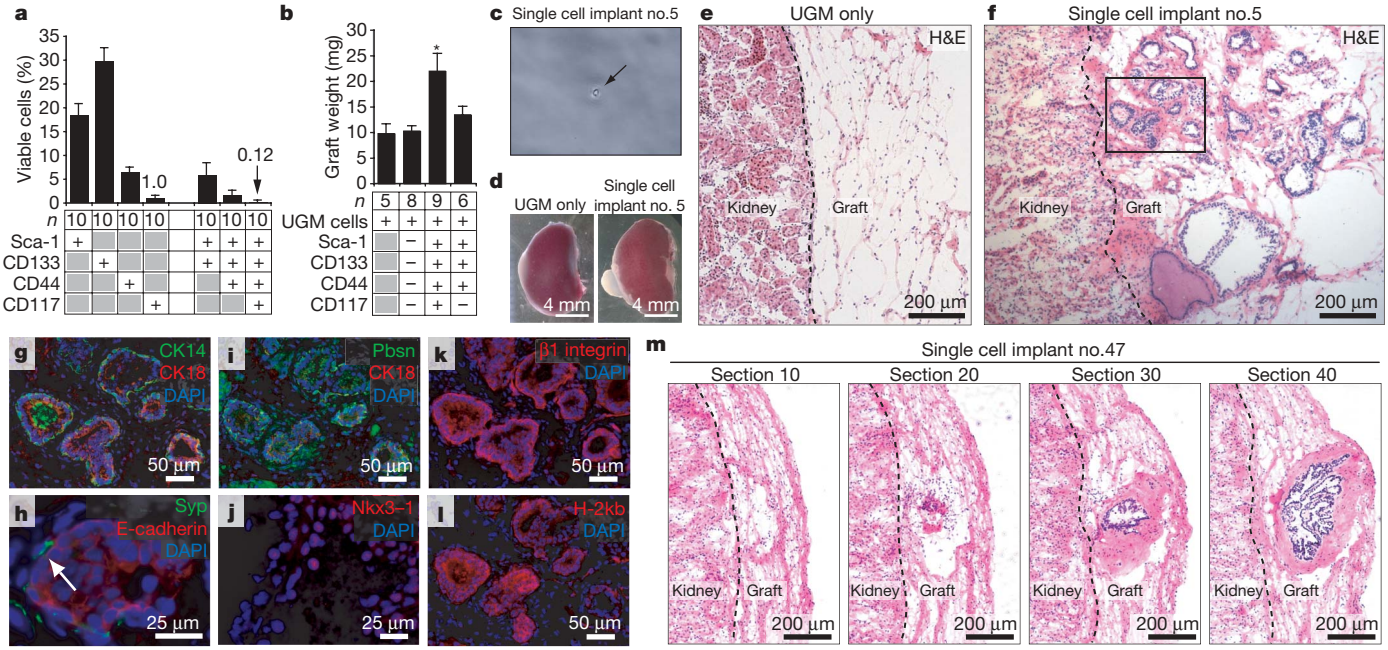

Figure 3 | A single adult stem cell with the phenotype Lin$^-$Sca-1$^+$CD133$^+$CD44$^+$CD117$^+$ can generate a secretion-producing prostate. **a**, Percentage of viable cells in the adult C57BL/6 prostate expressing single and multiple markers of prostate stem cells. **b**, Quantification of graft weight three months after renal capsule implantation. Data are from two independent experiments. *, Lin$^-$Sca-1$^+$CD133$^+$CD44$^+$CD117$^+$ versus Lin$^-$Sca-1$^-$CD133$^-$CD44$^-$CD117$^-$: $P = 0.002$; Lin$^-$Sca-1$^+$CD133$^+$CD44$^+$CD117$^+$ versus Lin$^-$Sca-1$^+$CD133$^+$CD44$^+$CD117$^-$: $P = 0.03$; Lin$^-$Sca-1$^+$CD133$^+$CD44$^+$CD117$^+$ versus UGM only: $P = 0.004$. **c**, Image of the single viable Lin$^-$Sca-1$^+$CD133$^+$CD44$^+$CD117$^+$ cell used for single cell implant no. 5 (indicated by an arrow). **d**, Prostate generation capacities of UGM only and Lin$^-$Sca-1$^+$CD133$^+$CD44$^+$CD117$^+$ single cell implant no. 5 three months after renal capsule implantation. **e**, Haematoxylin and eosin (H&E) stain of a UGM-only graft. Dotted line indicates the edge of the kidney parenchyma. **f**, Haematoxylin and eosin stain of single cell implant no. 5. Dotted line indicates the edge of the kidney parenchyma. **g–l**, Serial sections of the boxed area are shown stained for (**g**) CK14 (green), CK18 (red) and DAPI (blue), (**h**) Syp (green), E-cadherin (also known as Cdh1; red) and DAPI (blue; arrow indicates a Syp$^+$ cell), (**i**) Pbsn (green), CK18 (red) and DAPI (blue), (**j**) Nkx3-1 (red) and DAPI (blue), (**k**) β1 integrin (red) and DAPI (blue), and (**l**) H-2k^b (red) and DAPI (blue). **m**, Haematoxylin and eosin stain of single cell implant no. 47. Serial sections 10, 20, 30 and 40 are shown. Dotted line indicates the edge of the kidney parenchyma. All bars represent the mean and s.e.m.

haplotype H-2k^b antibody (Fig. 2j) that specifically recognizes donor (C57BL/6) but not host (athymic nu/nu) mouse cells (Supplementary Fig. 5). These findings demonstrate that the CD117$^+$ population is enriched for normal PSCs with functional prostate generation capacity.

To evaluate the self-renewal capacity of CD117$^+$ cells—a defining characteristic of stem cells[22]—and to determine whether decreased amounts of CD117$^+$ cells would retain prostate generation capacity, we performed serial transplantations with successively reduced numbers of CD117$^+$ cells (Supplementary Fig. 6a). Secondary and tertiary transplants of CD117$^+$ cells, but not CD117$^-$ cells, gave rise to functional prostates comprised of multiple cell types derived from donor C57BL/6 mouse cells (Supplementary Fig. 6b–q). These findings provide direct evidence that the CD117$^+$ population contains normal PSCs with self-renewal capacity.

We next determined whether CD117 signalling was important for normal prostate development. Mouse prostate development begins with epithelial budding from the urogenital sinus at 17.5 days of gestation, with extensive ductal outgrowth and branching occurring during the first 3 weeks of postnatal development[11]. Mice homozygous for the dominant-white spotting locus (W/W) lack CD117 signalling and are perinatal lethal[23], thus precluding an assessment of prostate development. We therefore analysed heterozygous W/W^v mice, which are viable and have partially impaired CD117 signalling[23]. At 4 weeks of age, despite an equivalent body size the mutant prostates were decreased in size with a similar reduction in adulthood (Supplementary Fig. 7a–d). We next examined cell proliferation, differentiation and survival in mutant prostates, because CD117 signalling regulates these processes in various stem cells[24]. Mutant prostates showed inhibited proliferation, although basal and luminal differentiation, cell survival and vascular/smooth muscle cell recruitment were unaltered (Supplementary Fig. 7e–h). Similarly, wild-type C57BL/6 prostates cultured *ex vivo* in the presence of a function-blocking anti-CD117 antibody (ACK2) showed inhibited growth and reduced branching (Supplementary Fig. 8a–c). We confirmed that ACK2 inhibited CD117 signalling by assessing the expression of Slug (also known as Snai2; Supplementary Fig. 8d–f)—a downstream target of the CD117 pathway[25]. Notably, treated prostates showed attenuated proliferation and an increased basal-to-luminal cell ratio, with no effect on cell survival (Supplementary Fig. 8g–l). To evaluate further a possible role for CD117 in PSC function *in vivo*, we administered ACK2 to castrated C57BL/6 mice at an *in vivo* inhibitory dose[26] and assessed prostate regeneration after hormone replacement. Attenuating CD117 function *in vivo* inhibited prostate regeneration concordant with inhibited proliferation and an increased basal-to-luminal cell ratio, with no effect on cell survival or vascular/smooth muscle cell recruitment (Supplementary Fig. 9a–i). These findings suggest that the impairment of CD117 signalling using antagonistic blockers, in contrast to the partial impairment as seen in W/W^v mice, may inhibit prostatic luminal cell differentiation and highlight a potential role for CD117 signalling in normal prostate development. Because CD117 signalling is important for bone-marrow-derived cellular function (including haematopoietic stem and endothelial progenitor cell mobilization[27]) and the vasculature and its supporting stroma may establish a PSC niche[14], it is possible that abrogated CD117 function may adversely affect non-epithelial cell recruitment/maintenance in the prostate, which in turn could compromise prostate development. Although we did not observe deficient vascular/smooth muscle cell recruitment in CD117 mutant and ACK2-treated mice, our studies do not rule out possible effects of abrogated CD117 signalling on non-epithelial cells in the prostate. Studies investigating the prostate-specific

©2008 Macmillan Publishers Limited. All rights reserved

conditional ablation of CD117 are needed to demonstrate conclusively a functional requirement for CD117 in normal prostate development.

To compare the percentage of CD117$^+$ cells in the prostate with that of other PSC populations, we obtained a lineage-depleted (Lin$^-$) population and performed flow cytometry. Whereas CD117$^+$ cells had the lowest frequency in the viable cell population (~1%), Sca-1$^+$ and CD133$^+$ cells were detected at much higher frequencies (Fig. 3a). Indeed, other studies have reported Sca-1 and CD133 expression in both stem and non-stem-cell types, including stromal and differentiated epithelial cells[7,28]. These higher frequencies suggest that Sca-1 and CD133 may mark heterogeneous subpopulations of prostate cells. Given the heterogeneity of single-stained cell populations, we would not expect each marker used alone to yield a subpopulation composed entirely of stem cells. We therefore performed fluorescence-activated cell sorting (FACS) to obtain cell populations expressing combinations of multiple surface markers (Supplementary Fig. 10), followed by renal capsule implantation. We determined that PSCs resided exclusively within the Lin$^-$Sca-1$^+$CD133$^+$CD44$^+$CD117$^+$ population, which constituted 0.12% of the viable cell population (pgf: Lin$^-$Sca-1$^-$CD133$^-$CD44$^-$CD117$^-$, 0/8; Lin$^-$Sca-1$^+$CD133$^+$CD44$^+$CD117$^+$, 6/9; Lin$^-$Sca-1$^+$CD133$^+$CD44$^+$CD117$^-$, 0/6; Fig. 3a, b and Supplementary Fig. 11a–h). Serial transplantation yielded similar results (pgf: Lin$^-$Sca-1$^-$CD133$^-$CD44$^-$CD117$^-$, 0/3; Lin$^-$Sca-1$^+$CD133$^+$CD44$^+$CD117$^+$, 1/3; Lin$^-$Sca-1$^+$CD133$^+$CD44$^+$CD117$^-$, 0/3; Supplementary Fig. 12a–f). Hence the Lin$^-$Sca-1$^+$CD133$^+$CD44$^+$CD117$^+$ population contains normal PSCs with self-renewal capacity.

To definitively prove that prostate generation could be achieved from a single Lin$^-$Sca-1$^+$CD133$^+$CD44$^+$CD117$^+$ cell, we sorted single viable cells into individual wells, imaged each well to confirm the presence of a single cell, and grafted single donor C57BL/6 mouse cells in combination with rat UGM stromal cells under the renal capsule of host athymic nu/nu mice (Supplementary Fig. 13). A total of 14 prostates were generated from 97 single cell transplants (Fig. 3c, d). Histological analyses confirmed that whereas grafts of UGM cells alone were incapable of prostate generation (Fig. 3e), grafts of the 14 successful single cell transplants showed substantial prostate development (Fig. 3f). We confirmed the presence of epithelial tubules comprised of multiple cell lineages (Fig. 3g, h) as well as the expression of Pbsn (Fig. 3i) and Nkx3-1 (Fig. 3j). Notably, single-cell-derived prostates expressed mouse-specific β1 integrin (Fig. 3k) and C57BL/6 donor-specific H-2k^b (Fig. 3l). We further confirmed the donor origin of the generated prostates by PCR-based genotyping of laser capture microdissected cells (Supplementary Fig. 14a). Single-cell-derived prostates had an interconnected branching morphology surrounded by a layer of stromal cells and connective tissue (Fig. 3m). By limiting dilution analysis, the frequency of PSCs in the Lin$^-$Sca-1$^+$CD133$^+$CD44$^+$CD117$^+$ population was calculated as 1 in 10 (Supplementary Fig. 14b).

To determine whether CD117 would also mark a potential PSC population in the human prostate, we performed flow cytometric analysis of human benign prostatic hyperplasia (BPH; $n = 5$) and benign non-BPH ($n = 4$) specimens. CD117$^+$ cells were observed at a low frequency in the viable cell population in benign non-BPH and BPH specimens (~0.2% and 0.4%, respectively; Fig. 4a, b). By combining multiple stem cell markers, we determined the frequency of viable CD133$^+$CD44$^+$CD117$^+$ cells (a Sca-1 human orthologue has not been identified) in benign non-BPH and BPH specimens to be 0.004% and 0.01%, respectively (Fig. 4a, b). Immunostaining revealed CD117$^+$ cells in the prostate epithelium that co-expressed the basal marker p63 in both benign non-BPH (Fig. 4c–e) and BPH (Fig. 4f–h) specimens. These findings suggest that CD117 expression, in addition to marking a PSC population in the mouse prostate, may also mark a potential PSC population in the human prostate. *In vivo* prostate generation from human CD117$^+$ prostate cells, however, remains to be demonstrated.

This is, to our knowledge, the first report to demonstrate prostate generation from a single adult stem cell. Recently, two studies described mouse mammary gland reconstitution from a single stem cell[29,30]. By demonstrating that a functional organ could be generated from a single adult stem cell, these studies signified hallmark advancement in the stem cell research field. Our study now adds to this advancement. Determining the phenotype of stem cells with single cell tissue generation capacity has important implications for

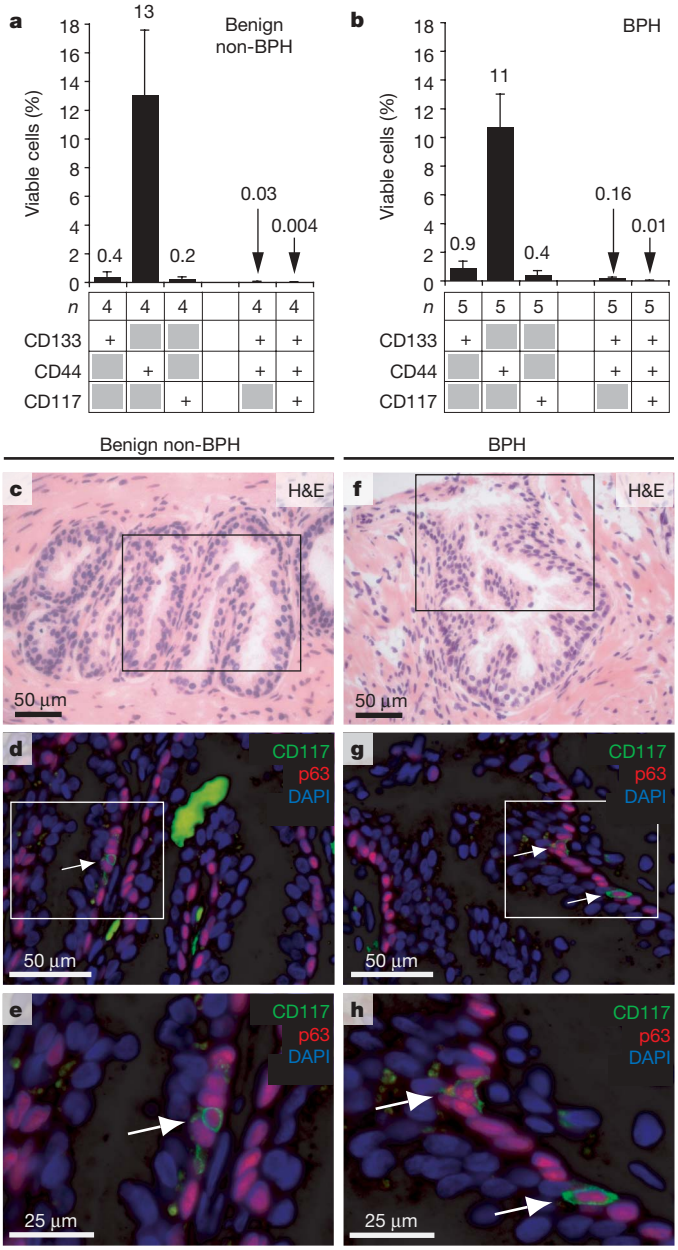

Figure 4 | Human prostates contain a subpopulation of CD117$^+$ cells that localize to the basal layer of the prostate epithelium. **a**, **b**, Percentage of viable cells in human clinical benign non-BPH prostate specimens (**a**) or human clinical BPH prostate specimens (**b**) expressing single and multiple markers of prostate stem cells. **c**–**h**, Histological analyses of a benign non-BPH prostate specimen (**c**–**e**) and a BPH prostate specimen (**f**–**h**) stained for haematoxylin and eosin (H&E) (**c**, **f**) and CD117 (green), p63 (red) and DAPI (blue) (**d**, **e**, **g**, **h**). The boxed areas in **c** and **f** are shown enlarged in **d** and **g**, respectively, and the boxed areas in **d** and **g** are shown enlarged in **e** and **h**, respectively. Arrows indicate cells co-expressing CD117 and p63. All bars represent the mean and s.e.m. The benign non-BPH and BPH specimens used for histological analyses were paired specimens taken from the same patient.

©2008 Macmillan Publishers Limited. All rights reserved

tissue repair and regrowth and for cancer stem/initiating cell identification.

METHODS SUMMARY

Prostate generation *in vivo*. The prostate generation assay was described previously[17,18]. For primary transplants of $CD117^+$ cells, prostates from 8–10-week-old C57BL/6 mice were dissociated and magnetically sorted with anti-mouse CD117 microbeads (Miltenyi Biotec) into $CD117^{+/-}$ fractions (~500,000 dissociated cells were obtained per prostate, with $CD117^+$ cells constituting 7% of magnetically sorted cells, of which $17.5 \pm 2.4\%$ ($n = 10$) were viable as determined by flow cytometry). Sorted cells (100,000 cells per graft) were mixed with UGM stromal cells (250,000 cells per graft) in 3 mg ml^{-1} collagen type I (20 μl per graft), incubated at 37 °C for 1 h to allow collagen gelation, and overlaid with prostate culture medium. After incubation overnight at 37 °C, collagen gels were grafted under the renal capsule of 6–8-week-old athymic nu/nu mice, along with a subcutaneous 90-day slow-release testosterone pellet (12.5 mg per pellet per mouse; Innovative Research of America). Grafts were collected 8 weeks after implantation. For primary transplants of $Lin^-Sca\text{-}1^+CD133^+CD44^+CD117^+$ cells, prostates were sorted by FACS, and the sorted cells (1,300 cells per graft) were mixed with UGM stromal cells (250,000 cells per graft). Grafts were collected 12 weeks after implantation.

Single cell FACS and prostate generation *in vivo*. Details of the procedure are described in Supplementary Fig. 13. Prostates from 8–10-week-old C57BL/6 mice were dissociated and lineage-depleted using a Mouse Lineage Cell Depletion Kit (Miltenyi Biotec), along with a biotin-conjugated anti-mouse CD31 monoclonal antibody (BD Biosciences; clone 390). FACS was performed with a FACSAria flow cytometer (Becton Dickinson). Compensation adjustments were performed with single colour positive controls. Single cells were sorted into Microtest U-bottom 96 well plates (BD Falcon) containing 20 μl collagen type I at 3 mg ml^{-1}. A total of 127 individual wells from single cell FACS were examined, with 106 wells verified to contain a single viable cell from six independent experiments.

Full Methods and any associated references are available in the online version of the paper at www.nature.com/nature.

Received 25 January; accepted 16 September 2008.
Published online 22 October 2008.

1. Isaacs, J. T. in *Control of Cell Proliferation and Cell Death in the Normal and Neoplastic Prostate. Benign Prostatic Hyperplasia* (eds C. H. Rodgers *et al.*) Vol. II 85–94 (National Institutes of Health, Report No. 87–2881, 1987).
2. Abate-Shen, C. & Shen, M. M. Molecular genetics of prostate cancer. *Genes Dev.* **14,** 2410–2434 (2000).
3. Burger, P. E. *et al.* Sca-1 expression identifies stem cells in the proximal region of prostatic ducts with high capacity to reconstitute prostatic tissue. *Proc. Natl Acad. Sci. USA* **102,** 7180–7185 (2005).
4. Liu, A. Y. *et al.* Cell–cell interaction in prostate gene regulation and cytodifferentiation. *Proc. Natl Acad. Sci. USA* **94,** 10705–10710 (1997).
5. Richardson, G. D. *et al.* CD133, a novel marker for human prostatic epithelial stem cells. *J. Cell Sci.* **117,** 3539–3545 (2004).
6. Tsujimura, A. *et al.* Prostatic stem cell marker identified by cDNA microarray in mouse. *J. Urol.* **178,** 686–691 (2007).
7. Xin, L., Lawson, D. A. & Witte, O. N. The Sca-1 cell surface marker enriches for a prostate-regenerating cell subpopulation that can initiate prostate tumorigenesis. *Proc. Natl Acad. Sci. USA* **102,** 6942–6947 (2005).
8. Collins, A. T., Habib, F. K., Maitland, N. J. & Neal, D. E. Identification and isolation of human prostate epithelial stem cells based on $\alpha_2\beta_1$-integrin expression. *J. Cell Sci.* **114,** 3865–3872 (2001).
9. Lawson, D. A., Xin, L., Lukacs, R. U., Cheng, D. & Witte, O. N. Isolation and functional characterization of murine prostate stem cells. *Proc. Natl Acad. Sci. USA* **104,** 181–186 (2007).
10. Schmelz, M. *et al.* Identification of a stem cell candidate in the normal human prostate gland. *Eur. J. Cell Biol.* **84,** 341–354 (2005).
11. Sugimura, Y., Cunha, G. R. & Donjacour, A. A. Morphogenesis of ductal networks in the mouse prostate. *Biol. Reprod.* **34,** 961–971 (1986).
12. Salm, S. N. *et al.* TGF-β maintains dormancy of prostatic stem cells in the proximal region of ducts. *J. Cell Biol.* **170,** 81–90 (2005).
13. Tsujimura, A. *et al.* Proximal location of mouse prostate epithelial stem cells: a model of prostatic homeostasis. *J. Cell Biol.* **157,** 1257–1265 (2002).
14. Wang, G. M., Kovalenko, B., Wilson, E. L. & Moscatelli, D. Vascular density is highest in the proximal region of the mouse prostate. *Prostate* **67,** 968–975 (2007).
15. Bonkhoff, H. & Remberger, K. Differentiation pathways and histogenetic aspects of normal and abnormal prostatic growth: a stem cell model. *Prostate* **28,** 98–106 (1996).
16. Signoretti, S. *et al.* p63 is a prostate basal cell marker and is required for prostate development. *Am. J. Pathol.* **157,** 1769–1775 (2000).
17. Cunha, G. R. & Lung, B. The possible influence of temporal factors in androgenic responsiveness of urogenital tissue recombinants from wild-type and androgen-insensitive (Tfm) mice. *J. Exp. Zool.* **205,** 181–193 (1978).
18. Xin, L., Ide, H., Kim, Y., Dubey, P. & Witte, O. N. *In vivo* regeneration of murine prostate from dissociated cell populations of postnatal epithelia and urogenital sinus mesenchyme. *Proc. Natl Acad. Sci. USA* **100,** 11896–11903 (2003).
19. Kurita, T., Medina, R. T., Mills, A. A. & Cunha, G. R. Role of p63 and basal cells in the prostate. *Development* **131,** 4955–4964 (2004).
20. Johnson, M. A., Hernandez, I., Wei, Y. & Greenberg, N. Isolation and characterization of mouse probasin: An androgen-regulated protein specifically expressed in the differentiated prostate. *Prostate* **43,** 255–262 (2000).
21. Shen, M. M. & Abate-Shen, C. Roles of the *Nkx3.1* homeobox gene in prostate organogenesis and carcinogenesis. *Dev. Dyn.* **228,** 767–778 (2003).
22. Weissman, I. L. Stem cells: units of development, units of regeneration, and units in evolution. *Cell* **100,** 157–168 (2000).
23. Lev, S., Blechman, J. M., Givol, D. & Yarden, Y. Steel factor and c-*kit* protooncogene: genetic lessons in signal transduction. *Crit. Rev. Oncog.* **5,** 141–168 (1994).
24. Ashman, L. K. The biology of stem cell factor and its receptor C-kit. *Int. J. Biochem. Cell Biol.* **31,** 1037–1051 (1999).
25. Perez-Losada, J. *et al.* Zinc-finger transcription factor Slug contributes to the function of the stem cell factor c-kit signaling pathway. *Blood* **100,** 1274–1286 (2002).
26. Moss, K. G., Toner, G. C., Cherrington, J. M., Mendel, D. B. & Laird, A. D. Hair depigmentation is a biological readout for pharmacological inhibition of KIT in mice and humans. *J. Pharmacol. Exp. Ther.* **307,** 476–480 (2003).
27. Heissig, B., Werb, Z., Rafii, S. & Hattori, K. Role of c-kit/Kit ligand signaling in regulating vasculogenesis. *Thromb. Haemost.* **90,** 570–576 (2003).
28. Shmelkov, S. V. *et al.* CD133 expression is not restricted to stem cells, and both $CD133^+$ and $CD133^-$ metastatic colon cancer cells initiate tumors. *J. Clin. Invest.* **118,** 2111–2120 (2008).
29. Shackleton, M. *et al.* Generation of a functional mammary gland from a single stem cell. *Nature* **439,** 84–88 (2006).
30. Stingl, J. *et al.* Purification and unique properties of mammary epithelial stem cells. *Nature* **439,** 993–997 (2006).

Supplementary Information is linked to the online version of the paper at www.nature.com/nature.

Acknowledgements We thank J. Cupp, L. Gilmour and W. Tombo for FACS support, X.-D. Wang, R. Soriano and Z. Modrusan for microarray services, I. Kasman, L. Komuves and J. Eastham-Anderson for microscopy assistance, B. D. Tarlow for assistance with laser-capture microdissection and PCR-based genotyping, Genentech Laboratory Animal Resources for support services, L. Blocher and J. Simko for human clinical prostate specimens, and F. J. de Sauvage for valuable discussion, input and supervision of the project.

Author Contributions K.G.L. planned the project, designed and performed experiments, and prepared the manuscript. B.-E.W. assisted with *ex vivo* prostate studies. L.J. provided input and supervised the project. W.-Q.G. conceptualized the study, planned and supervised the project. All authors discussed the results and commented on the manuscript.

Author Information Reprints and permissions information is available at www.nature.com/reprints. Correspondence and requests for materials should be addressed to W.-Q.G. (gao@gene.com).

©2008 Macmillan Publishers Limited. All rights reserved

METHODS

Animals. Pregnant SD rats and C57BL/6 male mice (postnatal day 4 and 8–10-weeks-old) were purchased from Charles River Laboratories, athymic nu/nu male mice (6–8-weeks-old) were purchased from Harlan Sprague Dawley, and WBB6F1/J male mice (wild type or W/W^v; 4–8-weeks-old) were purchased from the Jackson Laboratory. The W allele encodes a *Cd117* gene with a deletion of the transmembrane domain and the amino terminus of the kinase domain, whereas the W^v allele encodes a *Cd117* gene with a single point mutation. All experiments were approved by the Animal Research Ethics Committee of Genentech.

Human prostate clinical specimens. Freshly resected human prostate specimens (both BPH and benign non-BPH specimens, distinguished by gross examination by a pathologist; wet weights between 1 and 3 g) were obtained from Bio-options Inc. and The University of California, San Francisco, from consenting patients in accordance with federal and state guidelines.

Antibodies. Antibodies were purchased from the following sources: BD Biosciences, allophycocyanin (APC)-conjugated CD117 (anti-mouse: clone 2B8; anti-human: clone YB5.B8), phycoerythrin (PE)-Cy7-conjugated Sca-1 (clone D7), Ki67 (clone B56), E-cadherin (clone 36), active caspase 3 (polyclonal 557035); eBioscience, PE-conjugated CD133 (anti-mouse: clone 13A4), APC-Alexa Fluor 750-conjugated CD44 (anti-mouse/human: clone IM7), function-blocking CD117 (clone ACK2); Miltenyi Biotec, PE-conjugated CD133 (anti-human: clone AC133); Abcam, CK18 (clone C-04), H-2k^b (clone ER-HR52), CD117 (polyclonal ab956); Chemicon, mouse-specific β1 integrin (clone MB1.2), synaptophysin (clone SY38); R&D Systems, CD117 (clone 180627); Covance, CK14 (polyclonal AF64); AbD Serotec, CD31 (clone 2H8); Sigma, α-smooth muscle actin (SMA) (clone 1A4); Santa Cruz Biotechnology, probasin (polyclonal M-18), p63 (clone 4A4); Invitrogen, synaptophysin (polyclonal Z66), secondary antibodies conjugated to Alexa Fluor 488 or 594. Nkx3-1 polyclonal antibody was a gift from C. Abate-Shen.

UGM stromal cell preparation. The UGM isolation procedure has been described previously[18]. In brief, E18 embryos from pregnant SD rats were killed and urogenital sinuses were collected. After separation of the UGM from the urogenital sinus epithelium, the UGM was digested with 1 mg ml^{-1} collagenase/dispase (Roche) in DMEM supplemented with 10% fetal bovine serum (FBS), 2 mM glutamine, 100 U ml^{-1} penicillin and 100 mg ml^{-1} streptomycin for 60 min at 37 °C, washed twice in prostate culture medium (DMEM supplemented with 10% FBS, 2 mM glutamine, 10 μg ml^{-1} insulin, 5.5 μg ml^{-1} transferrin, 6.7 ng ml^{-1} selenium, 1 nM testosterone (Innovative Research of America), 100 U ml^{-1} penicillin and 100 mg ml^{-1} streptomycin) and cultured in the same medium in 24-well plates coated with 10 μg ml^{-1} collagen type I. UGM cells were passaged at confluency by trypsin digestion and cultured *in vitro* for up to 1 week.

Prostate cell preparation. Human and mouse prostates were minced, placed in DMEM supplemented with 10% FBS, 2 mM glutamine, 100 U ml^{-1} penicillin and 100 mg ml^{-1} streptomycin, digested with 1 mg ml^{-1} collagenase/dispase for 90 min at 37 °C with agitation and passed through a 70 μm filter.

Serial isolation/transplantation *in vivo*. For secondary transplants of CD117$^+$ cells, primary grafts were magnetically sorted (~49,000 dissociated cells were obtained per primary graft, with CD117$^+$ cells constituting 19% of magnetically sorted cells), and sorted cells (10,000 cells per graft) were mixed with UGM stromal cells (250,000 cells per graft). For tertiary transplants of CD117$^+$ cells, secondary grafts were magnetically sorted (~40,000 dissociated cells were obtained per secondary graft, with CD117$^+$ cells constituting 11% of magnetically sorted cells) and sorted cells (2,200 cells per graft) were mixed with UGM stromal cells (250,000 cells per graft). For secondary transplants of Lin$^-$Sca-1$^+$CD133$^+$CD44$^+$CD117$^+$ cells, primary grafts were sorted by FACS (~31,000 dissociated cells were obtained per secondary graft, with Lin$^-$Sca-1$^+$CD133$^+$CD44$^+$CD117$^+$ cells constituting 0.02% of viable FACS-sorted cells). Sorted cells (15 cells per graft) were mixed with UGM stromal cells (250,000 cells per graft). All serial transplantation grafts were collected 12 weeks after implantation. Gross graft images were acquired on a SMZ 800 dissecting microscope (Nikon) with a Coolpix 4300 digital camera (Nikon).

RNA isolation and qRT–PCR. Prostates from 8–10-week-old C57BL/6 mice were collected and teased apart to extend the tubules. For comparison of prostatic regions, each prostatic lobe was divided into distal, intermediate and proximal regions. For comparison of prostatic lobes, each prostate was divided into dorsal, lateral, ventral and anterior lobes. Total RNA was isolated using an RNeasy Mini kit (Qiagen) and qRT–PCR was performed with Power SYBR Green (Applied Biosystems) using the following primer sets: *Sca-1*, 5′-ATGGACACTTCTCACACTACAAAG-3′ and 5′-TCAGAGCAAGGTCTGCAGGAGGACTG-3′; *Cd44*, 5′-AATTCCGAGGATTCATCCCA-3′ and 5′-CGCTGCTGACATCGTCATC-3′; *Cd49b*, 5′-CCGGCATACGAAAGAATTGG-3′ and 5′-GAAGAGCTGAGGGTTATGT-3′; *Cd49f* (also known as *Itga6*), 5′-GTGGCCCAAGGAGATTAGC-3′ and 5′-GTTGACGCTGCAGTTGAGA-3′; *Cd133*, 5′-ACCAACACCAAGAACAAGGC-3′ and 5′-GGAGCTGACTTGAATTGAGG-3′; *Bcl2*, 5′-ATGTGTGTGGAGAGCGTCAAC-3′ and 5′-AGACAGCCAGGAGAAATCAAAC-3′; *Tert*, 5′-ATGGCGTTCCTGAGTATG-3′ and 5′-TTCAACCGCAAGACCGACAG-3′; *p63*, 5′-TTGTACCTGGAAAACAATG-3′ and 5′-TCGAAGCTGTGTGGGCCCGGG-3′; *Ck14*, 5′-GACTTCCGGACCAAGTTTGA-3′ and 5′-CTTGAGGCTCTCAATCTGC-3′; *Ck18*, 5′-ACTCCGCAAGGTGGTAGATG-3′ and 5′-GCCTCGATTTCTGTCTCCAG-3′; *Cd24*, 5′-TAAAGGACGCGTGAAAGGTTTGA-3′ and 5′-GACAAAATGGGTCTCCATTCCGCAC-3′; *Cd34*, 5′-ATGCAGGTCCACAGGGACACG-3′ and 5′-CTGTCCTGATAGATCAAGTAG-3′; *Cd117*, 5′-GACGCAACTTCCTTATGATC-3′ and 5′-TGGTTTGAGCATCTTCACGG-3′; *Slug*, 5′-TTTCTCCAGACCCTGGCTGCT-3′ and 5′-TTTTCCCCAGTGTGAGTTCTA-3′; *Gapdh*, 5′-ACTGGCATGGCCTTCCG-3′ and 5′-CAGGCGGCACGTCAGATC-3′. Gene expression was normalized to *Gapdh* using the ΔC_T method.

Flow cytometry. Prostate cells (non-lineage depleted) were permeabilized with 0.1% Triton X-100, stained with primary (CK14, CK18, APC-conjugated CD117) and secondary (Alexa Fluor 488 or 594) antibodies, and analysed on an LSR-II flow cytometer (Becton Dickinson).

Colony formation *in vitro*. The prostate colony formation assay has been described previously[13]. In brief, prostate cells from 8–10-week-old C57BL/6 mice were magnetically sorted into CD117$^{+/-}$ fractions, resuspended at 8,000 cells per 100 μl collagen type I at 3 mg ml^{-1} in DMEM, placed in flat-bottom 96-well plates for 1 h at 37 °C, and overlaid with prostate culture medium supplemented with 15 ng ml^{-1} epidermal growth factor (Roche). Medium was changed every 48 h and colony formation was assessed after 7 days.

Prostate culture *ex vivo*. Postnatal day 4 C57BL/6 mouse prostates were collected and placed on 8-μm pore-size cell culture inserts (BD Falcon), and inserts were placed into 24-well plates containing 300 μl DMEM/F-12 supplemented with 0.5% glucose, 2 mM glutamine, 10 μg ml^{-1} insulin, 5.5 μg ml^{-1} transferrin, 6.7 ng ml^{-1} selenium, 100 U ml^{-1} penicillin, 100 mg ml^{-1} streptomycin, and 25 ng ml^{-1} fungizone. Medium supplemented with function-blocking anti-CD117 antibody (25 μg ml^{-1}) was also used. Medium was changed and images were acquired every 48 h, and prostates were collected after 10 days. Images were acquired on a MZ16FA dissecting microscope (Leica) with a Retiga EXi digital camera (QImaging). Net growth in prostate area was quantified using MetaMorph software (Molecular Devices). Branch point quantification was performed on gross images of day 8 prostates.

Castration and androgen replacement. For microarray and qRT–PCR analysis, C57BL/6 mice at 8–10 weeks of age were used. On day 0, mice were castrated. On days 3 and 14 after castration, prostates from a subset of mice were collected. On day 14 after castration, testosterone pellets (15 mg per pellet per mouse) were implanted, and on day 17 (3 days after hormone replacement) prostates were collected. Total RNA was isolated using an RNeasy Mini kit and MOE430v2 Affymetrix chips were used for microarray analysis. To assess CD117 function during prostate regeneration *in vivo*, C57BL/6 mice at 8 weeks of age were used. Mice were castrated on day 0, and on day 12 after castration anti-ragweed control antibody (10 mg kg^{-1} in PBS) or function-blocking anti-CD117 antibody (10 mg kg^{-1} in PBS) were administered by intraperitoneal injection. On day 14 after castration testosterone pellets (15 mg per pellet per mouse) were implanted and on day 15 (1 day after hormone replacement) antibody treatments were administered. On day 19 (5 days after hormone replacement) prostates were collected, weighed and processed for histology. Prostate weights are expressed as the net increase compared to control prostates from day 14 after castration.

Immunohistochemistry. Optimal cutting temperature (OCT) compound-frozen tissues were sectioned at 8 μm, fixed in 4% paraformaldehyde (for CK14, CK18, CD117, Syp, Pbsn, β1 integrin, H-2k^b, CD31 and SMA) or methanol/acetone (1:1 (v/v); for E-cadherin, active caspase3, Ki67 and Nkx3-1), and incubated with primary antibody for 45 min and secondary antibody for 30 min. Human prostate specimens were fixed in formalin and sectioned at 6 μm, and antigen retrieval was performed with BD Retrievagen A (BD Biosciences). For specificity controls, species-matched primary antibodies were used. Images were acquired on an Axioplan 2 imaging microscope (Zeiss) with an ORCA-ER digital camera (Hamamatsu). For *ex vivo* prostates, percentages of positive cells were quantified by assessing at least 600 cells for CK14 or CK18, 400 cells for Ki67 and 1,200 cells for E-cadherin. For regenerated *in vivo* prostates, the percentages of positive cells were quantified by assessing at least 800 cells for CK14 or CK18 and 2,500 cells for Ki67.

Laser capture microdissection and PCR-based genotyping. Single-cell-derived grafts were sectioned at 8 μm, mounted on metal frame membrane slides (Molecular Machines & Industries) and stained with mouse-specific β1 integrin and CD31. Within the graft, β1 integrin$^+$CD31$^-$ cells were isolated with a Nikon E2000 CellCut laser capture microdissector (Molecular Machines & Industries).

©2008 Macmillan Publishers Limited. All rights reserved

For *Foxn1*$^{+/+}$ cell controls, rat stromal cells (β1 integrin^{-}CD31^{-}) within the graft were isolated. For *Foxn1*$^{+/-}$ cell controls, athymic nu/nu kidney cells (β1 integrin^{+}) adjacent to the graft were isolated. Captured cells were lysed with a PicoPure DNA Extraction Kit (Molecular Devices) and PCR-based genotyping was performed (http://jaxmice.jax.org/pub-cgi/protocols/protocols.sh). Genomic DNA was amplified by PCR with primers for *Foxn1* (5'-GGCCCAGCAGGCAGCCCAAG-3′ and 5′-AGGGATCTCCTCAAAGGCT-TC-3′), digested with BsaJI and run on a 4% agarose gel. The undigested PCR product is 168 base pairs (bp); the digested *Foxn1*$^{+/+}$ PCR product gives 90-, 58- and 20-bp fragments; the digested *Foxn1*$^{+/-}$ PCR product gives 110-, 90-, 58- and 20-bp fragments. The absence of a 110-bp product indicates that genomic DNA is derived from *Foxn1*$^{+/+}$ (wild type) cells. PCR control reactions included water (negative control) and wild-type mouse genomic DNA (positive control).

Confocal and single cell microscopy. Confocal images were scanned and acquired with a LSM 510 META confocal microscope (Zeiss). Single cell images were acquired on an Eclipse TE300 inverted microscope (Nikon) with a Cascade Photometrics digital camera (Roper Scientific).

Limiting dilution analysis. Limiting dilution analysis was performed using the 'limdil' function in the 'statmod' software package (http://bioinf.wehi.edu.au/software/limdil/index.html). A confidence interval of 95% was used.

Statistical analysis. Group differences were evaluated using a two-tailed Student's *t*-test. *P* values of less than 0.05 were considered significant.

©2008 Macmillan Publishers Limited. All rights reserved